Intestinal epithelial MHC class II regulation by HDAC3 instructs microbiota-specific CD4+ T cells

Emily M. Eshleman[1,3], Tzu-Yu Shao[2,3,4], Vivienne Woo[1,3], Taylor Rice[1,3], Jordan Whitt[1,3], Laura Engleman[1,3], Sing Sing Way[2,3], and Theresa Alenghat[1,3]

[1]Division of Immunobiology, [2]Division of Infectious Disease, [3]Center for Inflammation and Tolerance, [4]Immunology Graduate Program, Cincinnati Children's Hospital Medical Center and the University of Cincinnati College of Medicine, Cincinnati, OH 45229 USA

Abstract

Aberrant immune responses to resident microbes promote inflammatory bowel disease and other chronic inflammatory conditions. However, how microbiota-specific immunity is controlled in mucosal tissues remains poorly understood. Here, we find that mice lacking epithelial expression of microbiota-sensitive histone deacetylase 3 (HDAC3) exhibit increased accumulation of commensal-specific $CD4^+$ T cells in the intestine, provoking the hypothesis that epithelial HDAC3 may instruct local microbiota-specific immunity. Consistent with this, microbiota-specific $CD4^+$ T cells and epithelial HDAC3 expression were concurrently induced following early-life microbiota colonization. Further, epithelial-intrinsic ablation of HDAC3 promoted T cell driven-colitis and primed development of pathogenic commensal-specific Th17 cells. Mechanistically, HDAC3 was essential for MHC class II (MHCII) expression by the intestinal epithelium, and epithelial-intrinsic MHCII actively limited commensal-specific Th17 cells and prevented microbiota-triggered inflammation. Remarkably, HDAC3 enabled the microbiota to induce MHCII on epithelial cells and limit the number of commensal-specific T cells in the intestine. Collectively, these data reveal a central role for an epithelial histone deacetylase in controlling development of tissue-intrinsic T cells that recognize commensal microbes and drive pathologic inflammation.

Introduction

The gastrointestinal tract is home to trillions of microorganisms, collectively termed the microbiota, which form symbiotic relationships with mammalian cells and play a significant role in mediating health and disease. Extensive experiments utilizing broad-spectrum antibiotics or germ-free (GF) mouse models have revealed the necessity for the microbiota in the development and function of the host immune system (1–4). Microbiota interactions are particularly impactful during early-life, as critical immune education and calibration occur within the first few years of life (5–8). Indeed, disturbances or perturbations in microbiota composition or colonization during this early-life window have been associated with long-lasting changes in immunity that can predispose to the development of chronic inflammatory disorders including asthma, allergy, and inflammatory bowel diseases (IBD) (1, 4, 7).

Despite the symbiotic nature of the host-microbiota relationship, the close association and abundance of microbes at mucosal surfaces pose a potential risk to stimulate pathologic inflammation. This requires that intestinal immune responses must be tightly regulated to allow protective immunity against invading pathogens, while limiting inflammatory responses towards innocuous commensal microbes. Commensal bacteria drive regulatory T cell differentiation (9), and microbiota-reactive effector and memory T cells are present in both mice and humans (10–14). These commensal-specific T cells promote barrier function by inducing protective cytokines and providing cross-reactivity to pathogens (13, 15, 16). However, aberrant immune responses to the microbiota also trigger inflammatory conditions, such as IBD (1, 17–19). In mouse models of colitis, intestinal microbes drive inflammation, in part, by stimulating microbiota-reactive $CD4^+$ T cells (20–22). Further, microbiota-specific $CD4^+$ T cells in IBD patients have been shown to be functionally altered and produce more pro-inflammatory cytokines such as IL-17, compared to T cells from healthy patients (13, 23–27). However, the mechanisms instructing tissue-intrinsic regulation of commensal-specific $CD4^+$ T cells remains poorly understood.

80 Intestinal epithelial cells (IECs) reside at the direct interface between the microbiota and
81 immune cells, and are thus uniquely poised to instruct local immunity in response to
82 microbial antigens. IECs express pathogen recognition receptors that sense microbial
83 signals and regulate intestinal immune responses via secretion of cytokines,
84 chemokines, and growth factors (1, 28). While specialized microfold cells and goblet
85 cell-associated antigen passages in the epithelium deliver antigens to underlying
86 antigen presenting myeloid cells (29–31), IECs are also equipped with classical antigen
87 processing and presentation pathways that can regulate immune responses (32, 33).
88 However, there remains limited understanding of IEC-directed mechanisms that
89 coordinate healthy microbiota-immune relationships.
90
91 Beyond canonical sensors, epithelial expression of the epigenetic-modifying enzyme
92 histone deacetylase 3 (HDAC3) has recently been found to respond to the microbiota
93 and regulate mammalian metabolism, intestinal homeostasis, and inflammation (34–37).
94 Here, we found that microbiota-dependent expansion of commensal-specific $CD4^+$ T
95 cells following initial microbiota colonization occurred concurrently with epithelial
96 expression of HDAC3. Given this relationship, we examined whether IEC-intrinsic
97 HDAC3 regulates antigen specificity directed to the microbiota. Indeed, loss of HDAC3
98 expression in IECs resulted in intestinal inflammation and accumulation of microbiota-
99 specific Th17 cells that were regulated by epithelial MHCII. Interestingly, germ-free
100 analyses demonstrated that HDAC3 was necessary for microbiota to induce epithelial
101 MHCII-dependent regulation of microbiota-specific T cells. Taken together, these data
102 reveal that the microbiota induce commensal tolerance and limit inflammation by
103 directing epithelial control of tissue-intrinsic T cells.
104
105 **Results**
106 **Epithelial HDAC3 expression limits commensal-specific $CD4^+$ T cells in the**
107 **intestine.** Microbiota colonization begins at birth with the complexity and density of the
108 microbiota increasing most significantly during infancy (38–40). Microbiota exposure
109 early in life is required for effective immune education and disruption during this window

110 can increase chronic inflammatory disorders (39–43). While it has been predicted that
111 initial colonization at birth must direct development of local T cell specificity to
112 commensal microbes, this has not been directly tested. Therefore, to investigate
113 whether early-life microbiota colonization itself instructs commensal-specific T cell
114 responses in the intestine, $CD4^+$ T cells from the large intestine of germ-free (GF) and
115 conventionally-housed (CNV) neonatal pups were first analyzed for specificity to
116 microbial antigens using MHCII-tetramers loaded with commensal-flagella peptide,
117 cBir1. Within the first week of life, GF and CNV pups exhibited a similarly low
118 abundance of commensal-specific $cBir1^+$ $CD4^+$ T cells in the large intestine (**Figure 1, A**
119 **and B**). However, microbiota colonization increases by weaning (41) and, interestingly,
120 3-week old pups reared in the presence of microbes already demonstrated an
121 accumulation of $cBir1^+$ $CD4^+$ T cells compared to age-matched GF controls (**Figure 1, A**
122 **and B**). Thus, as predicted, early microbiota-derived signals are essential for initial
123 expansion of intestinal microbiota-specific $CD4^+$ T cells.
124
125 Dysregulated commensal-specific T cells accumulate in patients with intestinal
126 inflammation (13), suggesting that impairment in pathways that regulate these T cell
127 subsets can impact susceptibility to pathologic inflammation. Interestingly, IECs from
128 IBD patients express decreased levels of the HDAC3 enzyme (34) and, consistent with
129 findings in other facilities (34), mice lacking IEC-intrinsic expression of HDAC3
130 ($HDAC3^{\Delta IEC}$ mice) displayed increased susceptibility to chronic intestinal inflammation
131 (34) characterized by rectal prolapse (**Supplemental Figure 1A**), increased levels of
132 the inflammatory biomarker, lipocalin-2 (**Supplemental Figure 1B**), infiltration of
133 inflammatory cells (**Supplemental Figure 1, C-E**), and pathology consistent with
134 chronic inflammation (**Supplemental Figure 1F**). Strikingly, epithelial expression of
135 HDAC3 was also dramatically induced in 3-week old pups relative to younger 1-week
136 old pups (**Figure 1C**). However, age-matched pups raised under GF conditions
137 demonstrated low epithelial HDAC3 expression that was unaltered with age (**Figure**
138 **1C**), indicating that microbiota colonization increases early-life epithelial HDAC3
139 expression in the intestine.

140

141 The temporal link between epithelial-intrinsic HDAC3 expression and expansion of
142 commensal-specific $CD4^+$ T cells following microbiota colonization provoked the
143 hypothesis that IEC-intrinsic HDAC3 may regulate microbiota-specific T cell immunity.
144 In the intestinal lamina propria, total $CD3^+$ T cells were unaltered in $HDAC3^{\Delta IEC}$ mice
145 compared to wildtype floxed littermate controls ($HDAC3^{FF}$) (**Figure 1D**). Interestingly,
146 though, loss of epithelial HDAC3 resulted in elevated intestinal $CD4^+$ T cells, but not
147 $CD8a^+$ cells, (**Figure 1, E and F**) that exhibited increased $cBir1^+$ commensal-specificity
148 (**Figure 1, H and I**). These $cBir1^+$ $CD4^+$ T cells were characterized by a higher
149 frequency of pro-inflammatory $ROR\gamma t^+$ Th17 cells in $HDAC3^{\Delta IEC}$ mice compared to
150 floxed controls (**Figure 1, J and K**). Taken together, these data indicate that epithelial
151 HDAC3 plays a critical role in regulating intestinal microbiota-specific Th17 cells.
152

153 **$CD4^+$ T cells from mice lacking epithelial HDAC3 induce severe colitis.** To
154 determine whether dysregulated $CD4^+$ T cells in $HDAC3^{\Delta IEC}$ mice promoted intestinal
155 inflammation, the T cell transfer model of chronic colitis was employed in which purified
156 $CD4^+$ T cells were isolated from $HDAC3^{FF}$ and $HDAC3^{\Delta IEC}$ mice and transferred into
157 $Rag1^{-/-}$ mice (**Figure 2A**). In contrast to $Rag1^{-/-}$ recipients who received $CD4^+$ T cells
158 from control mice, $Rag1^{-/-}$ recipients receiving $CD4^+$ T cells from $HDAC3^{\Delta IEC}$ mice
159 displayed more significant weight loss (**Figure 2B**), colonic shortening (**Figure 2C**), and
160 severe colitis pathology characterized by inflammatory cell infiltration, crypt hyperplasia,
161 and mural thickening (**Figure 2, D and E**). Furthermore, luminal concentration of the
162 inflammatory biomarker, lipocalin-2, was also significantly upregulated in $Rag1^{-/-}$ mice
163 that received $CD4^+$ T cells from $HDAC3^{\Delta IEC}$ mice (**Figure 2F**). Therefore, $CD4^+$ T cells
164 from mice that specifically lack IEC-intrinsic HDAC3 are sufficient to induce intestinal
165 inflammation in genetically-susceptible hosts.
166

167 To next investigate whether colitogenic T cells isolated from $HDAC3^{\Delta IEC}$ mice were
168 responding to commensal antigens, intestinal microbiota-reactive $CD4^+$ T cells were
169 evaluated. $Rag1^{-/-}$ recipients that received $CD4^+$ T cells from $HDAC3^{\Delta IEC}$ mice exhibited

170 elevated microbiota-specific cBir1^{+} CD4^{+} T cells compared to hosts that received
171 HDAC3^{FF} cells (**Figure 2, G and H**). In addition, a higher frequency of commensal-
172 specific T cells differentiated into inflammatory RORγt^{+} Th17 cells when they originated
173 from HDAC3$^{\Delta IEC}$ mice compared to HDAC3^{FF} littermate controls (**Figure 2I**). Collectively,
174 these data indicate that epithelial HDAC3 expression is required for regulation of CD4^{+}
175 T cell development in the intestine, as loss of epithelial HDAC3 resulted in increased
176 microbiota-specific colitogenic CD4^{+} T cells.
177
178 **HDAC3 regulates surface expression of MHC class II on intestinal epithelial cells.**
179 Antigen presentation via MHCII is critical for instructing antigen-specific CD4^{+} T cell
180 responses. However, the frequency of total MHCII^{+} intestinal hemopoietic cells (**Figure**
181 **3A**) and classical APCs, including MHCII^{hi} intestinal dendritic cells and macrophages,
182 were unaffected by epithelial HDAC3 deletion (**Figure 3, B and C**). Surprisingly, though,
183 we found that EpCAM^{+} IECs, and not CD45^{+} hematopoietic cells, expressed the
184 majority of MHCII at the intestinal-microbiota interface (**Figure 3, D and E**). IECs
185 respond to microbial cues, so we next assessed whether the microbiota plays a role in
186 regulating IEC-intrinsic MHCII expression. Consistent with other studies (44–48), IECs
187 isolated from CNV mice displayed higher surface expression of MHCII compared to GF
188 mice (**Figure 3, F and G**). Further, neonatal GF pups maintained low epithelial
189 expression of H2-Ab1, the gene which encodes the beta-chain of MHCII (**Figure 3H**).
190 However, epithelial H2-Ab1 expression was robustly induced following initial microbiota
191 colonization (**Figure 3H**), similar to regulation of HDAC3 (Figure 1C). These data
192 indicate the necessity of the microbiota in controlling IEC-intrinsic MHCII and suggest
193 that HDAC3 may regulate epithelial MHCII. Therefore, surface expression of MHCII
194 protein was compared on IECs isolated from the large intestine HDAC3^{FF} and
195 HDAC3$^{\Delta IEC}$ mice. Interestingly, loss of HDAC3 expression dramatically reduced MHCII
196 expression on IECs (**Figure 3, I and J**). These findings reveal a critical regulatory role
197 for HDAC3 in directing surface expression of MHCII on intestinal epithelial cells.
198

199 **Epithelial MHCII limits commensal-specific CD4$^+$ T cells and intestinal**
200 **inflammation.** While epithelial MHCII has been suggested to function in both protective
201 or detrimental immune responses (44, 48–50), its role in regulating commensal-specific
202 T cell responses and microbiota-triggered inflammation has not been directly examined.
203 Therefore, to test this, we generated an IEC-specific MHCII knockout model (MHCII$^{\Delta IEC}$)
204 by crossing floxed H2-Ab1 mice (MHCII^{FF}) to mice expressing Cre recombinase
205 downstream of the villin promoter (51, 52). Significant reduction in MHCII expression in
206 IECs of MHCII$^{\Delta IEC}$ mice was confirmed by mRNA (**Supplemental Figure 2A**) and
207 surface protein analyses (**Supplemental Figure 2B**) and, importantly, loss of MHCII
208 expression did not occur on CD45$^+$ cells in MHCII$^{\Delta IEC}$ mice (**Supplemental Figure 2C**).
209 In contrast to the activating role of MHCII on classical APCs, loss of IEC-intrinsic MHCII
210 led to elevated accumulation of commensal-specific cBir1$^+$ CD4$^+$ T cells in the colon of
211 MHCII$^{\Delta IEC}$ mice relative to floxed control mice (**Figure 4, A and B**). In order to examine
212 whether this commensal-specific response occurred with another microbial antigen,
213 mice were also colonized with *Candida albicans* expressing 2W1S$_{55\text{-}68}$ variant of I-Ea
214 epitope (**Figure 4C**) (53–55). Consistent with regulation of cBir1$^+$ CD4$^+$ T cells,
215 MHCII$^{\Delta IEC}$ mice displayed increased numbers of *C. albicans*-2W1S-specific CD4$^+$ T cells
216 relative to MHCII^{FF} mice (**Figure 4, D and E**) with similar levels of *C. albicans*
217 colonization. Collectively, these data reveal that IEC-intrinsic MHCII does in fact control
218 commensal-specific CD4$^+$ T cell levels in the intestine.
219
220 Mice lacking IEC-intrinsic HDAC3 exhibited increased susceptibility to chronic intestinal
221 inflammation (Figure S1). Remarkably, similar to HDAC3$^{\Delta IEC}$ mice, mice lacking
222 epithelial MHCII also displayed an increased incidence of rectal prolapse with age
223 (**Figure 4F**), indicative of intestinal inflammation. Furthermore, prolapsed MHCII$^{\Delta IEC}$
224 mice (MHCII$^{\Delta IEC*}$) demonstrated increased fecal lipocalin-2 (**Figure 4G**), pathology
225 consistent with chronic colitis (**Figure 4H**), and increased infiltration of myeloid cells
226 (**Figure 4, I and J**). Interestingly, MHCII$^{\Delta IEC}$ mice and HDAC3$^{\Delta IEC}$ mice with an
227 increased propensity to prolapse were characterized by elevated levels of commensal-
228 specific CD4$^+$ T cells (**Figure 4K**) that reflected commensal-specific RORγt$^+$

229 inflammatory Th17 cells (**Figure 4L**). Collectively, these data suggest that epithelial
230 HDAC3 may be critical in regulating microbiota-induced MHCII-directed commensal-
231 specific immunity and inflammation.
232
233 **HDAC3 enables microbiota to regulate epithelial dependent commensal-specific**
234 **immunity.** To test the requirement for the microbiota in MHCII-dependent intestinal
235 inflammation and commensal-specific immunity, MHCII^{FF} and MHCII$^{\Delta IEC}$ mice were
236 raised in the absence and presence of broad-spectrum antibiotics that significantly
237 deplete commensal bacteria (56). Consistent with earlier results (Figure 4F), MHCII$^{\Delta IEC}$
238 mice exhibited an increased prevalence of rectal prolapse (**Figure 5A**), whereas
239 depletion of the microbiota prevented spontaneous intestinal inflammation in MHCII$^{\Delta IEC}$
240 mice (**Figure 5A**). Furthermore, microbiota-replete MHCII$^{\Delta IEC}$ mice exhibited
241 accumulation of commensal-specific Th17 cells (**Figure 5B**) and increased levels of IL-
242 17 (**Figure 5C**). However, antibiotic-treated MHCII$^{\Delta IEC}$ mice did not demonstrate
243 increased commensal-specific Th17 cells (**Figure 5B**) or IL-17 expression (**Figure 5C**)
244 relative to MHCII^{FF} mice. Taken together, these data show that the microbiota is
245 necessary in triggering epithelial MHCII-dependent intestinal inflammation and
246 commensal-specific immune responses.
247
248 Therefore, to test whether HDAC3 is necessary in mediating this regulation of epithelial
249 and immune cells by the microbiota, GF-derived HDAC3^{FF} and HDAC3$^{\Delta IEC}$ mice were
250 compared to CNV-HDAC3^{FF} and HDAC3$^{\Delta IEC}$ mice. Consistent with earlier data
251 employing wildtype CNV and GF mice (Figure 3F, G), IEC-intrinsic MHCII expression
252 was significantly induced in CNV-HDAC3^{FF} controls compared to GF-HDAC3^{FF} mice
253 (**Figure 5, D and E**), whereas CNV-HDAC3$^{\Delta IEC}$ mice failed to upregulate MHCII (**Figure**
254 **5, D and E**). In GF mice, loss of epithelial HDAC3 expression had no impact on protein
255 levels of MHCII on IECs (**Figure 5, D and E**), demonstrating the specific necessity for
256 HDAC3 in mediating microbiota-dependent regulation of epithelial MHCII. Furthermore,
257 CNV-HDAC3$^{\Delta IEC}$ mice exhibited elevated cBir1^{+} commensal-specific Th17 cells
258 compared to CNV-HDAC3^{FF} littermate controls (**Figure 5, F and G**). However, GF-

259 HDAC3$^{\Delta IEC}$ had similar levels of commensal-specific Th17 cells as GF-HDAC3^{FF} mice
260 (**Figure 5, F and G)**. These data indicate the necessity for HDAC3 in enabling the
261 microbiota to regulate commensal-specific immunity. Collectively, these findings reveal
262 that microbiota colonization can induce commensal self-tolerance through an epithelial
263 HDAC3-MHCII regulatory pathway that dampens commensal-specific immune
264 responses directly in the local tissue environment (**Figure 5H**).
265
266 **Discussion**
267 The microbiota is essential for the development and education of the host immune
268 system. However, inappropriate immune reactions to the microbiota underlie several
269 chronic inflammatory conditions, highlighting the necessity to understand how
270 microbiota-specific immunity is controlled. In this study, we found that initial microbiota
271 colonization led to upregulation of epithelial HDAC3 expression and expansion of
272 commensal-specific T cells. Selective deletion of HDAC3 in IECs resulted in decreased
273 epithelial MHCII expression and impaired regulation of commensal-specific CD4^{+} T cells
274 that are controlled by epithelial MHCII. Importantly, these commensal-specific T cells
275 developed into Th17 cells that promote microbiota-triggered pathologic inflammation.
276 Furthermore, HDAC3 was necessary for microbiota to be able to induce epithelial
277 MHCII-dependent regulation of microbiota-specific T cells. Therefore, the microbiota
278 can direct self-tolerance by inducing a HDAC3-dependent epithelial MHCII pathway that
279 regulates local commensal-specific T cells and susceptibility to microbiota-sensitive
280 disease (**Figure 5H**).
281
282 Microbiota-specific CD4^{+} T cells are generated centrally in the thymus (57) and in
283 peripheral mucosal tissues (14, 58–60). While auto-reactive CD4^{+} T cell are well known
284 to be limited by thymic negative selection (61–63), the mechanisms controlling
285 commensal-specific cells remain less well understood. Previous work described that
286 negative selection of activated commensal-specific T cells can be mediated by MHCII-
287 expressing group 3 innate lymphoid cells (ILC3) (64, 65). While ILC3s are relatively
288 rare cells at the luminal surface of the intestine, we show that IECs are a major source

289 of intestinal MHCII. Indeed, HDAC3-dependent MHCII expression specifically by
290 epithelial cells limited accumulation of commensal-specific Th17 and thus, may be a
291 dominant mechanism at the luminal surface for controlling commensal-specific $CD4^+$ T
292 cells and dampening pathogenic responses to the microbiota. Given the role for MHCII
293 in ILC3s (64, 65), complementary and essential roles for antigen presentation pathways
294 in distinct non-classical cells seem to be crucial for establishing and maintaining healthy
295 intestine-intrinsic tissue homeostasis.
296
297 Loss of HDAC3-dependent epithelial MHCII led to elevated commensal-specific Th17
298 activity and increased susceptibility to microbiota-driven intestinal inflammation (**Figure**
299 **5H**). Patients with active IBD have functionally distinct microbiota-reactive $CD4^+$ T cells,
300 compared to those found in healthy controls, and secrete higher levels of IL-17 (13, 23,
301 25–27). IL-17 has been linked to development and exacerbation of several autoimmune
302 and inflammatory conditions, including IBD (25, 27, 66). Furthermore, mouse models
303 with disrupted IL-17 signaling are protected from intestinal inflammation (67, 68),
304 supporting a pathogenic role for IL-17 in intestinal inflammation. However, clinical trials
305 depleting IL-17 in IBD patients have been ineffective, and in some cases worsened
306 disease (69). This pleotropic role for IL-17 in regulating intestinal homeostasis suggests
307 that targeting specific IL-17 producers, instead of broadly neutralizing IL-17 itself, may
308 be a more effective treatment. In fact, work has shown that therapeutics which target
309 commensal-specific Th17 cells, while retaining IL-17 production from other cell types,
310 reduced intestinal inflammation (70). Our data suggests that promoting epithelial MHCII
311 expression through enhanced HDAC3 activity may further restrict pro-inflammatory
312 commensal-specific T cells and promote healthy intestinal homeostasis.
313
314 Crosstalk between the microbiota and mammalian immune cells involves
315 communication via pattern recognition receptor engagement and microbiota-derived
316 metabolite signaling. Our data reveal a distinct level of epithelial regulation in which the
317 microbiota-sensitive enzyme, HDAC3, regulates epithelial MHCII expression in the large
318 intestine. Indeed, loss of epithelial HDAC3 was sufficient to abrogate microbiota-

319 dependent MHCII expression in the intestine. Previous studies have linked the
320 requirement for the microbiota in regulating IEC-intrinsic MHCII expression (44–48).
321 Many of these studies have focused on how immune cells can induce epithelial MHCII
322 through IFNγ signaling (44, 71, 72). In addition, disruption to canonical pattern
323 recognition pathways leads to loss of intestinal barrier integrity and increased
324 inflammation (73–75), and the toll-like receptor signaling adaptors MyD88/TRAF have
325 been shown to induce epithelial MHCII expression, particularly in the small intestine
326 (44). However, whether crosstalk between microbiota-sensing pathways and/or IFNγ
327 signaling are required for HDAC3 regulation of epithelial MHCII and commensal-specific
328 immunity remains to be determined.
329
330 HDAC3 is a multifaceted enzyme that can deacetylate histone and non-histone targets
331 to alter gene expression and cellular functions. HDAC3 can be regulated by
332 endogenous factors, dietary components, and microbiota-derived signals (34, 35, 76–
333 78). While HDAC3 classically suppresses gene expression of direct targets via histone
334 deacetylation, more recent work has shown that HDAC3 may also function as a
335 transcriptional co-activator to induce gene expression through deacetylase-independent
336 activity (79–84). Given that H2-Ab1 expression is decreased in HDAC3$^{\Delta IEC}$ mice, loss of
337 HDAC3 may either directly increase expression of a repressor of H2-Ab1 or alter MHCII
338 expression through a secondary or non-histone target.
339
340 Increasing evidence suggests that several tissue-specific, non-hematopoietic cells,
341 including lung epithelial cells, skin keratinocytes, and fibroblasts express MHCII and the
342 necessary machinery to regulate tissue-intrinsic CD4^{+} T cell responses (85–87). Given
343 the ubiquitous nature of HDAC3, it is thus plausible that HDAC3 promotes MHCII-
344 dependent pathways in other non-classical antigen presenting cells as well.
345 Interestingly, tissue-specific deletion of HDAC3 has been associated with chronic
346 inflammatory disease models for diabetes, heart disease, Alzheimer's, and IBD (34, 35,
347 88–90). Importantly, our findings here uncover a fundamental new tenet for immune
348 regulation whereby HDAC3 induction of non-hematopoietic epithelial MHCII is largely

349 induced by the microbiota to dampen local self-directed immune responses. These
350 findings reveal a central host mechanism that is utilized by the microbiota to instruct
351 commensal-directed immunity, and suggest that this regulatory pathway can be
352 targeted to treat chronic inflammatory conditions.
353
354
355 **Methods**
356 ***Mice.*** Conventionally-housed C57Bl/6J mice were purchased from Jackson
357 Laboratories and maintained in our specific-pathogen free colony at Cincinnati
358 Children's Hospital Medical Center (CCHMC). Germ-free (GF) mice were maintained in
359 flexible isolators in the CCHMC Gnotobiotic Mouse Facility, fed autoclaved feed and
360 water, and monitored for absence of microbes. HDAC3^{FF} and HDAC3$^{\Delta IEC}$ were
361 generated as described (34). H2-Ab1(MHCII)^{FF} were purchased from Jackson and
362 maintained at CCHMC. MHCII^{FF} mice were crossed to C57BL/6J-Villin-Cre to generate
363 MHCII$^{\Delta IEC}$ mice. Sex- and age-matched littermate controls were used for all studies.
364 Mice were housed up to 4-per cage in a ventilated cage system in a 12-h light/dark
365 cycle, with free access to water and food. For T cell transfer colitis model, 5 x 10^5 naïve
366 CD4$^+$ T cells were isolated from the spleen and mesenteric lymph nodes of HDAC3^{FF}
367 and HDAC3$^{\Delta IEC}$ mice via the MojoSort Mouse CD4 Naïve T Cell Isolation (BioLegend).
368 Cell purity was confirmed by flow cytometry and T cells injected IP into age- and sex-
369 matched Rag1$^{-/-}$ recipients. *Candida albicans* colonization was conducted as previously
370 described (53, 54). Briefly, mice were pre-treated with ampicillin-water (1-mg/mL) two
371 days prior to colonization and maintained on ampicillin-water for the duration of the
372 experiment. Mice were gavaged with recombinant *C. albicans* expressing 2W1S$_{55-68}$
373 peptide (55). Mice were monitored for colonization by plating fecal CFUs and were
374 harvested 14-days post-colonization. For antibiotic treatment, MHCII^{FF} and MHCII$^{\Delta IEC}$
375 mice pups were provided water supplemented with 1-mg/mL colistin (Sigma), 1-mg/mL
376 ampicillin (Sigma) and 5-mg/mL streptomycin (Sigma) at weaning and maintained on
377 antibiotics for 16-weeks. Antibiotic-water was refreshed every 7-10 days. All mouse
378 studies were conducted with approval by Animal Care and Use Committees at CCHMC.

379 These protocols follow standards enacted by the United States Public Health Services
380 and Department of Agriculture. All experiments followed standards set forth by Animal
381 Research: Reporting of In Vivo Experiments (ARRIVE).
382
383 ***Cell Isolation.*** The large intestine was harvested, opened, and washed in PBS. For
384 IECs, tissue was placed in pre-warmed strip buffer (PBS, 5% FBS, 1mM EDTA, 1mM
385 DTT) and incubated at 37°C at 45-degree angle with shaking at 180-rpm for 15-min. For
386 lamina propria isolation, tissue was washed with PBS to remove EDTA and DTT then
387 incubated in pre-warmed digestion buffer (RPMI with 1-mg/mL Collagenase/Dispase
388 (Sigma)) at 37°C at 45-degree angle with shaking at 180-rpm for 30-min. After
389 incubation, the tissue was vortexed and passed through a 70μM cell strainer.
390
391 ***Flow cytometry.*** Cells were stained for flow cytometry using the following antibodies
392 diluted in FACS Buffer (2% FBS, 0.01% Sodium Azide, PBS): BV711-anti-CD326
393 (EpCAM) (Clone:G8.8, BioLegend), BUV395-anti-CD45.2 (Clone:104, BD Biosciences),
394 APC or FITC-anti-MHCII (Clone:M5/114.15.2, eBioscience), APC-eFluor-780-anti-CD4
395 (Clone:RM4-5, eBioscience), Pe-Cy7-anti-CD44 (Clone:IM7, eBioscience), AlexaFluor-
396 647-anti-RORγt (Clone:Q31-378, BD Biosciences), PerCP-eFluor710 or APC-anti-CD8a
397 (Clone:53-6.7, eBioscience), PerCP-Cy5.5-anti-CD3 (Clone: 17A2, eBioscience),
398 PerCP-eFluor710-anti-B220 (Clone:RA3-6B2, eBioscience), PerCP-eFluor710-anti-
399 Ly6G (Clone:1A8-Ly6g, eBioscience), PerCP-Cy5.5 or PE-anti-CD11b (Clone:M1/70,
400 eBioscience), PerCP-Cy5.5-anti-CD11c (Clone:N418, eBioscience). Dead cells were
401 excluded with the Fixable Aqua Dead Cell Stain Kit (Invitrogen). The BD Fix/Perm kit
402 was used for intracellular staining. Class-II restricted tetramers (cBir1 and 2W1S) were
403 PE-conjugated and were generated and provided by the NIH tetramer core. Samples
404 were acquired on the BD LSR-Fortessa and analyzed with FlowJo Software (Treestar).
405
406 ***RNA and qPCR analysis.*** RNA was isolated using the RNeasy Kit (Qiagen). For RNA
407 from whole tissue, samples were homogenized in TRIzol. Chloroform was added for
408 phase separation and RNA was precipitated by mixing with isopropanol. cDNA was

409 synthesized using the Verso reverse transcriptase kit (Thermo Fisher) following the
410 manufacturer's protocol. Real-time PCR was performed using SYBR green (Applied
411 Biosystems) and analyzed using the following murine primers sequences. HPRT
412 forward 5'- GATTAGCGATGAACCAGGT-3', HPRT reverse 5'-
413 CCTCCCATCTCCTTCATGACA-3', H2-Ab1 forward 5'-
414 TGTGAGTCCTGGTGACTGCCATTA-3', H2-Ab1 reverse 5'-
415 TCGCCCATGAACTGGTACACGAAA-3', IL-17 forward 5'-
416 ACCGCAATGAAGACCCTGAT-3', IL-17 reverse 5'- TCCCTCCGCATTGACACA-3',
417 HDAC3 forward 5'- TTGGTATCCTGGAGCTGCTT-3', HDAC3 Reverse 5'-
418 GACCCGGTCAGTGAGGTAGA-3'.
419
420 ***Lipocalin-2 ELISA.*** Fecal pellets were homogenized in PBS at a concentration of 100-
421 mg/mL then centrifuged at high-speed for 10-mins. Supernatants were collected and
422 lipocalin-2 levels were determined using mouse Lipocalin-2/NGAL (R&D Systems)
423 following the manufacturer's instructions.
424
425 ***Histological Analysis.*** Colonic tissue sections were fixed in 4% paraformaldehyde
426 overnight at 4°C then paraffin embedded, sectioned, and stained with hematoxylin and
427 eosin. For histological scoring, slides were evaluated based on the following
428 parameters: immune cell infiltration (1-5), mucosal thickening/edema (1-5), crypt length
429 (1-5), and crypt abscess/erosion (1-5).
430
431 ***Statistical analysis.*** Results are expressed as mean ± SEM. Statistical significance
432 was determined with the student's t-test or one-way ANOVA with all data meeting the
433 assumptions of the statistical test used. Results were considered significant at *$p <$
434 0.05; **$p < 0.01$; ***$p < 0.001$, ****$p < 0.0001$. Statistical significance was calculated
435 using Prism version 7.0 (GraphPad Software).
436

Author Contributions. Conceptualization, E.M.E., S.S.W., T.A.; Methodology, E.M.E, T.-Y.S., V.W., L.E., J.W., S.S.W., T.A.; Investigation, E.M.E., J.W., T.-Y.S., V.W., T.R.; Formal Analysis, E.M.E, T.-Y.S., T.R.; Writing, Review and Editing, E.M.E., S.S.W., T.A.

Acknowledgements. We thank the Way, Qualls, and Deshmukh labs for useful discussions and members of the Alenghat lab for critical reading of the manuscript. We thank CCHMC Veterinary Services, Research Flow Cytometry Core, Confocal Imaging Core, and Pathology Research Core for services and technical assistance. This research is supported by the National Institutes of Health (R01DK114123, R01DK116868 to T.A., DP1AI131080 to S.S.W, and F32AI147591 to E.M.E.), and a Kenneth Rainin Foundation award to T.A. S.S.W. and T.A. each hold Investigators in the Pathogenesis of Infectious Disease Award from the Burroughs Wellcome Fund. This project is supported in part by PHS grant P30DK078392.

452 **References**

453 1. Hill DA, Artis D. Intestinal bacteria and the regulation of immune cell homeostasis .
454 *Annu. Rev. Immunol.* 2010;28(1):623–667.

455 2. Belkaid Y, Harrison OJ. Homeostatic Immunity and the Microbiota . *Immunity*
456 2017;46(4):562–576.

457 3. Honda K, Littman DR. The microbiota in adaptive immune homeostasis and disease.
458 *Nature* 2016;535(7610):75–84.

459 4. Kayama H, Okumura R, Takeda K. Interaction between the Microbiota, Epithelia,
460 and Immune Cells in the Intestine. *Annu. Rev. Immunol.* 2020;38:23–48.

461 5. Koenig JE et al. Succession of microbial consortia in the developing infant gut
462 microbiome. *Proc. Natl. Acad. Sci. U. S. A.* 2011;108:4578–4585.

463 6. Yatsunenko T et al. Human gut microbiome viewed across age and geography.
464 *Nature* 2012;486(7402):222–227.

465 7. Zheng D, Liwinski T, Elinav E. Interaction between microbiota and immunity in health
466 and disease . *Cell Res.* 2020;30(6):492–506.

467 8. Bäckhed F et al. Dynamics and stabilization of the human gut microbiome during the
468 first year of life. *Cell Host Microbe* 2015;17(5):690–703.

469 9. Honda K, Littman DR. The Microbiome in Infectious Disease and Inflammation .
470 *Annu. Rev. Immunol.* 2012;30(1):759–795.

471 10. Duchmann R et al. T cell specificity and cross reactivity towards enterobacteria,
472 Bacteroides, Bifidobacterium, and antigens from resident intestinal flora in humans.
473 *Gut* 1999;44(6):812–818.

474 11. Duchmann R et al. Tolerance exists towards resident intestinal flora but is broken in
475 active inflammatory bowel disease (IBD). *Clin. Exp. Immunol.* 1995;102(3):448–455.

476 12. Ergin A et al. Impaired peripheral Th1 CD4+ T cell response to escherichia coli
477 proteins in patients with crohn's disease and ankylosing spondylitis. *J. Clin.*
478 *Immunol.* 2011;31(6):998–1009.

479 13. Hegazy AN et al. Circulating and Tissue-resident CD4+ T Cells With Reactivity to
480 Intestinal Microbiota Are Abundant in Healthy Individuals and Function is Altered
481 During Inflammation . *Gastroenterology* 2017;153(153):1320–1337.

482 14. Hand TW et al. Acute Gastrointestinal Infection Induces Long-Lived Microbiota-

483 Specific T Cell Responses . *Science (80-.).* 2012;337(6101):1553–1556.

484 15. Su LF, Kidd BA, Han A, Kotzin JJ, Davis MM. Virus-Specific CD4+ Memory-
485 Phenotype T Cells Are Abundant in Unexposed Adults . *Immunity* 2013;38(2):373–
486 383.

487 16. Campion SL et al. Proteome-wide analysis of HIV-specific naive and memory CD4+
488 T cells in unexposed blood donors. *J. Exp. Med.* 2014;211(7):1273–1280.

489 17. Kaser A, Zeissig S, Blumberg RS. Inflammatory Bowel Disease. *Annu. Rev.*
490 *Immunol.* 2010;28(12):573–621.

491 18. Tindemans I, Joosse ME, Samsom JN. Dissecting the Heterogeneity in T-Cell
492 Mediated Inflammation in IBD. *Cells* 2020;9(1):110.

493 19. Clemente JC, Ursell LK, Parfrey LW, Knight R. The impact of the gut microbiota on
494 human health: An integrative view. *Cell* 2012;148(6):1258–1270.

495 20. Belkaid Y, Bouladoux N, Hand TW. Effector and memory T cell responses to
496 commensal bacteria . *Trends Immunol.* 2013;34(6):299–306.

497 21. Maloy KJ, Powrie F. Intestinal homeostasis and its breakdown in inflammatory
498 bowel disease. *Nature* 2011;474(7351):298–306.

499 22. Cong Y et al. CD4+ T cells reactive to enteric bacterial antigens in spontaneously
500 colitic C3H/HeJBir mice: Increased T helper cell type 1 response and ability to
501 transfer disease. *J. Exp. Med.* 1998;187(6):855–864.

502 23. Annunziato F et al. Phenotypic and functional features of human Th17 cells. *J. Exp.*
503 *Med.* 2007;204(8):1849–1861.

504 24. Alexander M et al. Human gut bacterial metabolism drives Th17 activation and
505 colitis . *Cell Host Microbe* 2022;30(1):17-30.e9.

506 25. Gálvez J. Role of Th17 Cells in the Pathogenesis of Human IBD. *ISRN Inflamm.*
507 2014;2014:1–14.

508 26. Fujino S et al. Increased expression of interleukin 17 in inflammatory bowel disease.
509 *Gut* 2003;52(1):65–70.

510 27. Zhao J et al. Th17 Cells in Inflammatory Bowel Disease: Cytokines, Plasticity, and
511 Therapies. *J. Immunol. Res.* 2021;2021:8816041.

512 28. Eshleman EM, Alenghat T. Epithelial sensing of microbiota-derived signals . *Genes*
513 *Immun.* 2021;22(5–6):237–246.

514 29. Lo DD. Vigilance or Subversion? Constitutive and Inducible M Cells in Mucosal
515 Tissues. *Trends Immunol.* 2017;39(3):185–195.

516 30. Kulkarni DH et al. Goblet cell associated antigen passages support the induction
517 and maintenance of oral tolerance . *Mucosal Immunol.* 2020;13(2):271–282.

518 31. Kanaya T, Williams IR, Ohno H. Intestinal M cells: Tireless samplers of enteric
519 microbiota. *Traffic* 2020;21(1):34–44.

520 32. Biton M et al. T Helper Cell Cytokines Modulate Intestinal Stem Cell Renewal and
521 Differentiation . *Cell* 2018;175(5):1307-1320.e22.

522 33. Kambayashi T, Laufer TM. Atypical MHC class II-expressing antigen-presenting
523 cells: can anything replace a dendritic cell? . *Nat. Rev. Immunol.* 2014;14(11):719–
524 730.

525 34. Alenghat T et al. Histone deacetylase 3 coordinates commensal-bacteria-dependent
526 intestinal homeostasis. *Nature* 2013;504(7478):153–157.

527 35. Wu S en et al. Microbiota-derived metabolite promotes HDAC3 activity in the gut.
528 *Nature* 2020;586(7827):108–112.

529 36. Navabi N et al. Epithelial Histone Deacetylase 3 Instructs Intestinal Immunity by
530 Coordinating Local Lymphocyte Activation. *Cell Rep.* 2017;19(6):1165–1175.

531 37. Kuang Z et al. The intestinal microbiota programs diurnal rhythms in host
532 metabolism through histone deacetylase 3. *Science (80-.).* 2019;365(6460):1428–
533 1434.

534 38. Aagaard K, Stewart CJ, Chu D. Una destinatio, viae diversae. *EMBO Rep.*
535 2016;17(12):1679–1684.

536 39. Russell SL et al. Early life antibiotic-driven changes in microbiota enhance
537 susceptibility to allergic asthma. *EMBO Rep.* 2012;13(5):440–447.

538 40. Gensollen T, Iyer SS, Kasper DL, Blumberg RS. How colonization by microbiota in
539 early life shapes the immune system. *Science (80-.).* 2016;352(6285):539–544.

540 41. Al Nabhani Z et al. A Weaning Reaction to Microbiota Is Required for Resistance to
541 Immunopathologies in the Adult. *Immunity* 2019;50(5):1276-1288.e5.

542 42. Wang T et al. Early life antibiotic exposure and host health: Role of the microbiota–
543 immune interaction . *Semin. Perinatol.* 2020;44(8):151323.

544 43. Gray J et al. Intestinal commensal bacteria mediate lung mucosal immunity and

545 promote resistance of newborn mice to infection. *Sci. Transl. Med.* 2017;9(376):1–
546 14.

547 44. Koyama M et al. MHC Class II Antigen Presentation by the Intestinal Epithelium
548 Initiates Graft-versus-Host Disease and Is Influenced by the Microbiota. *Immunity*
549 2019;51(5):885-898.e7.

550 45. Matsumoto S et al. Gamma delta TCR-bearing intraepithelial lymphocytes regulate
551 class II major histocompatibility complex molecule expression on the mouse small
552 intestinal epithelium. *Epithelial Cell Biol.* 1995;4(4):163–170.

553 46. Umesaki Y, Okada Y, Matsumoto S, Imaoka A, Setoyama H. Segmented
554 filamentous bacteria are indigenous intestinal bacteria that activate intraepithelial
555 lymphocytes and induce MHC class II molecules and fucosyl asialo GM1 glycolipids
556 on the small intestinal epithelial cells in the ex-germ-free mouse. *Microbiol Immunol*
557 1995;39(8):555–62.

558 47. Matsumoto S et al. Physiological roles of γδ T-cell receptor intraepithelial
559 lymphocytes in cytoproliferation and differentiation of mouse intestinal epithelial
560 cells. *Immunology* 1999;97(1):18–25.

561 48. Tuganbaev T et al. Diet Diurnally Regulates Small Intestinal Microbiome-Epithelial-
562 Immune Homeostasis and Enteritis . *Cell* 2020;182(6):1441-1459.e21.

563 49. Jamwal DR et al. Intestinal Epithelial Expression of MHCII Determines Severity of
564 Chemical, T-Cell–Induced, and Infectious Colitis in Mice . *Gastroenterology*
565 2020;159(4):1342-1356.e6.

566 50. Thelemann C et al. Interferon-γ induces expression of MHC class II on intestinal
567 epithelial cells and protects mice from colitis. *PLoS One* 2014;9(1):1–10.

568 51. Hashimoto K, Joshi SK, Koni PA. A conditional null allele of the major
569 histocompatibility IA-beta chain gene. *Genesis* 2002;32(2):152–153.

570 52. El Marjou F et al. Tissue-specific and inducible Cre-mediated recombination in the
571 gut epithelium. *Genesis* 2004;39(3):186–193.

572 53. Jiang TT et al. Commensal Fungi Recapitulate the Protective Benefits of Intestinal
573 Bacteria . *Cell Host Microbe* 2017;22(6):809-816.e4.

574 54. Shao TY et al. Commensal Candida albicans Positively Calibrates Systemic Th17
575 Immunological Responses . *Cell Host Microbe* 2019;25(3):404-417.e6.

576 55. Igyártó BZ et al. Skin-Resident Murine Dendritic Cell Subsets Promote Distinct and
577 Opposing Antigen-Specific T Helper Cell Responses. *Immunity* 2011;35(2):260–272.

578 56. Vétizou M et al. Anticancer immunotherapy by CTLA-4 blockade relies on the gut
579 microbiota. *Science (80-.).* 2015;350(6264):1079–1084.

580 57. Zegarra-Ruiz DF et al. Thymic development of gut-microbiota-specific T cells .
581 *Nature* 2021;594(7863):413–417.

582 58. Belkaid Y, Hand TW. Role of the microbiota in immunity and inflammation. *Cell*
583 2014;157(1):121–141.

584 59. Xu M et al. c-MAF-dependent regulatory T cells mediate immunological tolerance to
585 a gut pathobiont . *Nature* 2018;554(7692):373–377.

586 60. Yang Y et al. Focused specificity of intestinal TH17 cells towards commensal
587 bacterial antigens . *Nature* 2014;510(7503):152–156.

588 61. Blackman M, Kappler J, Marrack P. The role of the T cell receptor in positive and
589 negative selection of developing T cells. *Science (80-.).* 1990;248(15):1335–1341.

590 62. Mathis D, Benoist C. Aire. *Annu. Rev. Immunol.* 2009;27:287–312.

591 63. Klein L, Kyewski B, Allen PM, Hogquist KA. Positive and negative selection of the T
592 cell repertoire: What thymocytes see (and don't see). *Nat. Rev. Immunol.*
593 2014;14(6):377–391.

594 64. Hepworth MR et al. Innate lymphoid cells regulate CD4+ T-cell responses to
595 intestinal commensal bacteria . *Nature* 2013;498(7452):113–117.

596 65. Hepworth MR et al. Group 3 innate lymphoid cells mediate intestinal selection of
597 commensal bacteria-specific CD4+ T cells . *Science (80-.).* 2015;348(6238):1031–
598 1035.

599 66. Ouyang W, Kolls JK, Zheng Y. The Biological Functions of T Helper 17 Cell Effector
600 Cytokines in Inflammation. *Immunity* 2008;28(4):454–467.

601 67. Schmidt EGW et al. TH17 cell induction and effects of IL-17A and IL-17F blockade
602 in experimental colitis. *Inflamm. Bowel Dis.* 2013;19(8):1567–1576.

603 68. Tang C et al. Suppression of IL-17F, but not of IL-17A, provides protection against
604 colitis by inducing T reg cells through modification of the intestinal microbiota . *Nat.*
605 *Immunol.* 2018;19(7):755–765.

606 69. Hueber W et al. Secukinumab, a human anti-IL-17A monoclonal antibody, for
607 moderate to severe Crohn's disease: unexpected results of a randomised, double-
608 blind placebo-controlled trial. *Gut* 2012;61(12):1693–1700.

609 70. Withers DR et al. Transient inhibition of ROR-γt therapeutically limits intestinal
610 inflammation by reducing TH17 cells and preserving group 3 innate lymphoid cells.
611 *Nat. Med.* 2016;22(3):319–323.

612 71. Blumberg RS et al. Antigen presentation by intestinal epithelial cells. . *Immunol.*
613 *Lett.* 1999;69(1):7–11.

614 72. Van Der Kraak LA et al. Genetic and commensal induction of IL-18 drive intestinal
615 epithelial MHCII via IFNγ . *Mucosal Immunol.* 2021;14(5):1100–1112.

616 73. Rakoff-Nahoum S, Pglino J, Eslami-Varzaneh F, Edberg S, Medzhitov R.
617 Recognition of comensal microflora by toll-like receptors in required for intestinal
618 homeostasis. *Cell* 2004;118:229–241.

619 74. Rhee SH et al. Pathophysiological role of Toll-like receptor 5 engagement by
620 bacterial flagenllin in colonic inflammation. *Proc. Natl. Acad. Sci. U. S. A.*
621 2005;102(38):13610–13615.

622 75. Rose WAI, Sakamoto K, Leifer CA. TLR9 is important for protection against
623 intestinal damage and for intestinal repair. *Sci. Rep.* 2012;2:1–9.

624 76. Haberland M, Montgomery RL, Olson EN. The many roles of histone deacetylases
625 in development and physiology: Implications for disease and therapy. *Nat. Rev.*
626 *Genet.* 2009;10(1):32–42.

627 77. Donohoe DR, Bultman SJ. Metaboloepigenetics: Interrelationships between energy
628 metabolism and epigenetic control of gene expression. *J. Cell. Physiol.*
629 2012;227(9):3169–3177.

630 78. Woo V, Alenghat T. Host – microbiota interactions : epigenomic regulation . *Curr.*
631 *Opin. Immunol.* 2017;44:52–60.

632 79. Chen X et al. Requirement for the histone deacetylase Hdac3 for the inflammatory
633 gene expression program in macrophages. *Proc. Natl. Acad. Sci. U. S. A.*
634 2012;109(42):2865–2874.

635 80. Greer CB et al. Histone Deacetylases Positively Regulate Transcription through the
636 Elongation Machinery . *Cell Rep.* 2015;13(7):1444–1455.

637 81. Lewandowski SL, Janardhan HP, Trivedi CM. Histone Deacetylase 3 coordinates
638 deacetylase-independent epigenetic silencing of transforming growth factor-β1
639 (TGF- β 1) to orchestrate second heart field development . *J. Biol. Chem.*
640 2015;290(45):27067–27089.

641 82. Emmett MJ et al. Histone deacetylase 3 prepares brown adipose tissue for acute

642 thermogenic challenge . *Nature* 2017;546(7659):544–548.

643 83. Wang Y et al. The intestinal microbiota regulates body composition through NFIL3
644 and the circadian clock. *Science (80-.).* 2017;916(357):912–916.

645 84. Nguyen HCB, Adlanmerini M, Hauck AK, Lazar MA. Dichotomous engagement of
646 HDAC3 activity governs inflammatory responses . *Nature* 2020;584(7820):286–290.

647 85. Tamoutounour S et al. Keratinocyte-intrinsic MHCII expression controls microbiota-
648 induced Th1 cell responses. *Proc. Natl. Acad. Sci. U. S. A.* 2019;116(47):23643–
649 23652.

650 86. Kerdidani D et al. Lung tumor MHCII immunity depends on in situ antigen
651 presentation by fibroblasts. *J. Exp. Med.* 2022;219(2). doi:10.1084/jem.20210815

652 87. Shenoy AT et al. Antigen presentation by lung epithelial cells directs CD4+ TRM cell
653 function and regulates barrier immunity. *Nat. Commun.* 2021;12(1).
654 doi:10.1038/s41467-021-26045-w

655 88. Feng D et al. A circadian rhythm orchestrated by histone deacetylase 3 controls
656 hepatic lipid metabolism. *Science (80-.).* 2011;331(6022):1315–1319.

657 89. Montgomery RL et al. Maintenance of cardiac energy metabolism by histone
658 deacetylase 3 in mice. *J. Clin. Invest.* 2008;118(11):3588–3597.

659 90. Ning L, Rui X, Bo W, Qing G. The critical roles of histone deacetylase 3 in the
660 pathogenesis of solid organ injury . *Cell Death Dis.* 2021;12(8):1–13.

661

662

663 **Figure Legends**

664

665 **Figure 1. Epithelial HDAC3 expression limits commensal-specific CD4$^+$ T cells in**
666 **the intestine.** (**A, B**) Number of cBir1$^+$ tetramer-specific CD4$^+$ T cells isolated from large
667 intestine of neonatal GF and CNV pups. (**C**) mRNA expression of HDAC3 in IECs
668 isolated from large intestine of GF and CNV pups. (**D**) Frequency of total intestinal
669 CD3$^+$. (**E**) Frequency of total intestinal CD8a$^+$ and (**F**) CD4$^+$ T cells. (**H, I**) Number of
670 cBir1$^+$ tetramer-specific CD4$^+$ T cells and (**J, K**) frequency of RORγt$^+$ cBir1$^+$ CD4$^+$ T cells
671 in large intestine of HDAC3^{FF} and HDAC3$^{\Delta IEC}$ mice. cBir1$^+$ tetramer cells are gated on
672 live, CD45$^+$, lineage (CD11b, B220, Ly6G, CD11c, CD8a)$^-$, CD4$^+$ cells. Data represent
673 at least two independent experiments, 3-4 mice per group. *p<0.05, **p<0.01, ns=not
674 significant.

675

676 **Figure 2. CD4$^+$ T cells from mice lacking epithelial HDAC3 induce severe colitis.**
677 (**A**) Experimental schematic of T cell colitis model with naïve CD4$^+$ T cells isolated from
678 HDAC3^{FF} and HDAC3$^{\Delta IEC}$ mice transferred into Rag1$^{-/-}$ hosts. (**B**) Change in body
679 weight, (**C**) colon length, (**D**) H&E-stained colonic sections of Rag1$^{-/-}$ hosts that received
680 T cells from HDAC3^{FF} or HDAC3$^{\Delta IEC}$ mice, scale bars 20 μM. (**E**) Histological scoring of
681 sections in (D). (**F**) Fecal concentration of lipocalin-2. (**G, H**) Number of cBir1$^+$ tetramer-
682 specific CD4$^+$ T cells in large intestine of Rag1$^{-/-}$ hosts that received T cells from
683 HDAC3^{FF} or HDAC3$^{\Delta IEC}$ mice. Gated on live, CD45$^+$, lineage (CD11b, B220, Ly6G,
684 CD11c, CD8a)$^-$, CD4$^+$. (**I**) Frequency of RORγt$^+$ cBir1$^+$ CD4$^+$ T cells. Data represent at
685 least two independent experiments, 3-4 mice per group. *p<0.05, **p<0.01.

686

687 **Figure 3. HDAC3 regulates surface expression of MHC class II on intestinal**
688 **epithelial cells.** (**A**) Frequency of total MHCII$^+$ cells in colon lamina propria. (**B, C**)
689 Frequency of dendritic cells and macrophages in large intestinal lamina propria of
690 HDAC3^{FF} and HDAC3$^{\Delta IEC}$ mice. Gated on live, CD45$^+$, MHCII$^+$. (**D**) MHCII$^+$ expressing
691 cells at colonic luminal surface. (**E**) Frequency of total MHCII$^+$ cells in (D). (**F, G**)
692 Frequency of MHCII$^+$ EpCAM$^+$ cells in large intestine of GF and CNV mice. (**H**) mRNA

693 expression of H2-Ab1 in IECs isolated from large intestine of GF and CNV pups. (**I, J**)
694 Frequency of MHCII^{+} EpCAM^{+} cells in large intestine of HDAC3^{FF} and HDAC3$^{\Delta IEC}$ mice.
695 Data represent at least three independent experiments, 3-4 mice per group. *p<0.05,
696 ***p<0.001, ****p<0.0001.
697
698 **Figure 4. Epithelial MHCII limits commensal-specific CD4^{+} T cells and intestinal**
699 **inflammation.** (**A, B**) Number of cBir1^{+}-specific CD4^{+} T cells in large intestine of
700 MHCII^{FF} and MHCII$^{\Delta IEC}$ mice. (**C**) Diagram of 2W1S-*Candida albicans* commensal
701 colonization. (**D, E**) Number of *C. albicans*-2W1S^{+}-specific CD4^{+} cells in large intestine
702 of MHCII^{FF} and MHCII$^{\Delta IEC}$ mice. (**F**) Frequency of rectal prolapse in MHCII^{FF} and
703 MHCII$^{\Delta IEC}$ mice. (**G**) Lipocalin-2 levels in stool of MHCII^{FF} and prolapsed MHCII$^{\Delta IEC}$ mice
704 (MHCII$^{\Delta IEC*}$). (**H**) H&E-stained colonic sections of MHCII^{FF} and MHCII$^{\Delta IEC*}$ mice, scale
705 bars 20 μM. (**I, J**) Frequency of myeloid cell infiltrate in MHCII^{FF} and MHCII$^{\Delta IEC*}$ mice.
706 (**K**) cBir1^{+}-specific CD4^{+} T cells and (**L**) frequency of RORγt^{+} cBir1^{+}-specific CD4^{+} T
707 cells in large intestine of control and prolapsed MHCII$^{\Delta IEC}$ and HDAC3$^{\Delta IEC}$ mice. Gated
708 on live, CD45^{+}, lineage (CD11b, B220, Ly6G, CD11c, CD8a)$^{-}$, CD4^{+}. Data are
709 representative of at least two independent experiments, 3-6 mice per group. *p<0.05,
710 **p<0.01, ***p<0.001.
711
712 **Figure 5. HDAC3 enables microbiota to regulate epithelial dependent commensal-**
713 **specific immunity.** (**A**) Frequency of rectal prolapse in control and antibiotic (ABX)-
714 treated MHCII^{FF} and MHCII$^{\Delta IEC}$ mice. (**B**) Frequency of RORγt^{+} cBir1^{+}-specific CD4^{+} T
715 cells and (**C**) IL-17 mRNA expression in large intestine of control and ABX-treated
716 MHCII^{FF} and MHCII$^{\Delta IEC}$ mice. (**D, E**) Frequency of MHCII^{+} EpCAM^{+} cells in large
717 intestine of GF- and CNV- HDAC3^{FF} and HDAC3$^{\Delta IEC}$ mice. (**F**) Number of cBir1^{+}
718 tetramer-specific CD4^{+} T cells and (**G**) frequency of RORγt^{+} cBir1^{+} T cells isolated from
719 GF- and CNV- HDAC3^{FF} and HDAC3$^{\Delta IEC}$ mice. cBir1^{+} tetramer cells are gated on live,
720 CD45^{+}, lineage (CD11b, B220, Ly6G, CD11c, CD8a)$^{-}$, CD4^{+}. (**H**) Microbiota drive self-
721 tolerance early in life through upregulation of an epithelial HDAC3 dependent-MHCII
722 pathway that limits commensal-specific Th17 cell accumulation and pathologic

723 inflammation. Data are representative of or pooled from at least two independent
724 experiments, 3-6 mice per group. *$p<0.05$, **$p<0.01$, ****$p<0.0001$, ns=not significant.
725

Figure 1

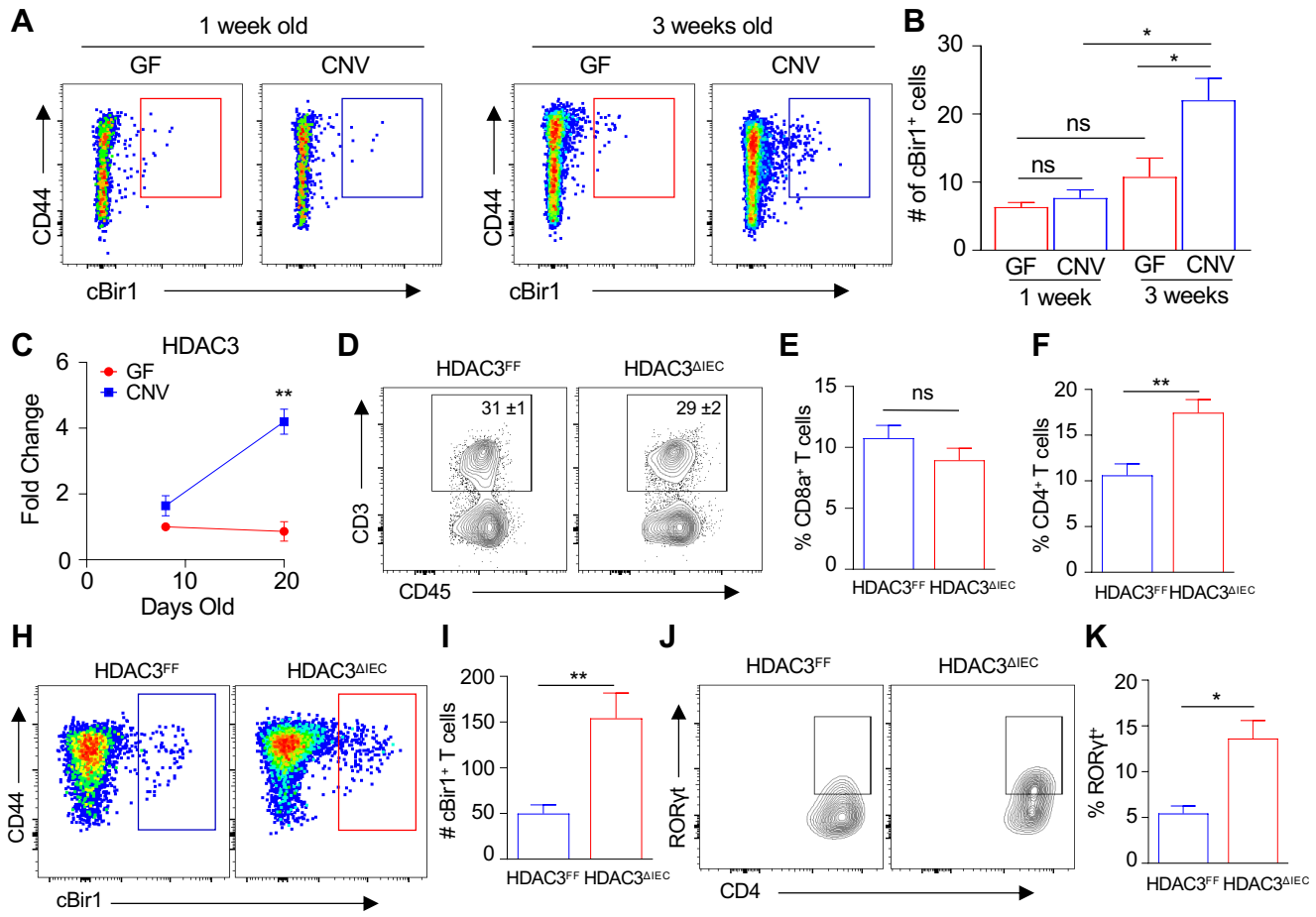

Figure. 1. Epithelial HDAC3 expression limits commensal-specific CD4+ T cells in the intestine. (**A, B**) Number of cBir1+ tetramer-specific CD4+ T cells isolated from large intestine of neonatal GF and CNV pups. (**C**) mRNA expression of HDAC3 in IECs isolated from large intestine of GF and CNV pups. (**D**) Frequency of total intestinal CD3+. (**E**) Frequency of total intestinal CD8a+ and (**F**) CD4+ T cells. (**H, I**) Number of cBir1+ tetramer-specific CD4+ T cells and (**J, K**) frequency of RORγt+ cBir1+ CD4+ T cells in large intestine of HDAC3FF and HDAC3ΔIEC mice. cBir1+ tetramer cells are gated on live, CD45+, lineage (CD11b, B220, Ly6G, CD11c, CD8a)-, CD4+. Data represent at least two independent experiments, 3-4 mice per group. *p<0.05, **p<0.01, ns=not significant.

Figure 2

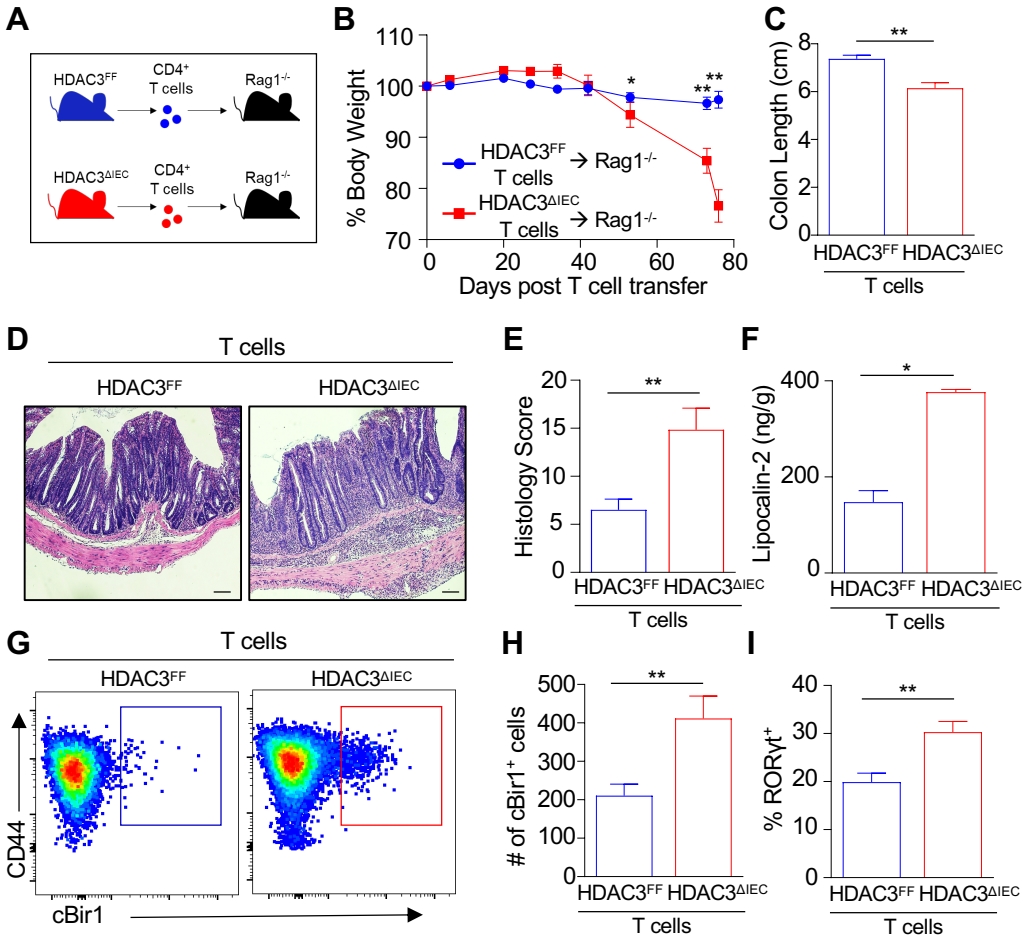

Figure. 2. CD4+ T cells from mice lacking epithelial HDAC3 induce severe colitis. (**A**) Experimental schematic of T cell colitis model with naïve CD4+ T cells isolated from HDAC3^{FF} and HDAC3$^{\Delta IEC}$ mice transferred into Rag1$^{-/-}$ hosts. (**B**) Change in body weight, (**C**) colon length, (**D**) H&E-stained colonic sections of Rag1$^{-/-}$ hosts that received T cells from HDAC3^{FF} or HDAC3$^{\Delta IEC}$ mice, scale bars 20 μM. (**E**) Histological scoring of sections in (D). (**F**) Fecal concentration of lipocalin-2. (**G, H**) Number of cBir1+ tetramer-specific CD4+ T cells in large intestine of Rag1$^{-/-}$ hosts that received T cells from HDAC3^{FF} or HDAC3$^{\Delta IEC}$ mice. Gated on live, CD45+, lineage (CD11b, B220, Ly6G, CD11c, CD8a)-, CD4+. (**I**) Frequency of RORγt+ cBir1+ CD4+ T cells. Data represent at least two independent experiments, 3-4 mice per group. *p<0.05, **p<0.01.

Figure 3

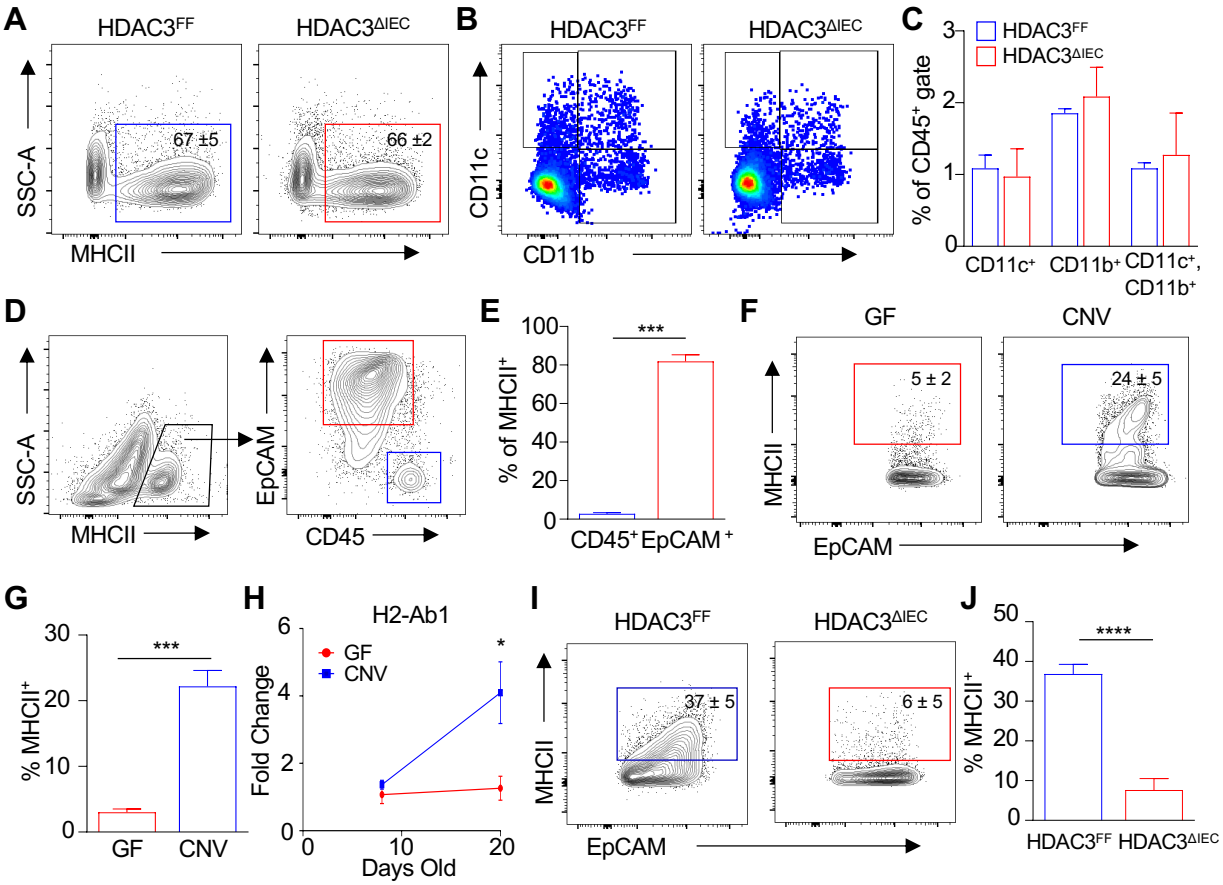

Figure. 3. HDAC3 regulates surface expression of MHC class II on intestinal epithelial cells. (**A**) Frequency of total MHCII+ cells in colon lamina propria. (**B, C**) Frequency of dendritic cells and macrophages in large intestinal lamina propria of HDAC3^{FF} and HDAC3$^{\Delta IEC}$ mice. Gated on live, CD45+, MHCII+. (**D**) MHCII+ expressing cells at colonic luminal surface. (**E**) Frequency of total MHCII+ cells in (D). (**F, G**) Frequency of MHCII+ EpCAM+ cells in large intestine of GF and CNV mice. (**H**) mRNA expression of H2-Ab1 in IECs isolated from large intestine of GF and CNV pups. (**I, J**) Frequency of MHCII+ EpCAM+ cells in large intestine of HDAC3^{FF} and HDAC3$^{\Delta IEC}$ mice. Data represent at least three independent experiments, 3-4 mice per group. *$p<0.05$, ***$p<0.001$, ****$p<0.0001$.

Figure 4

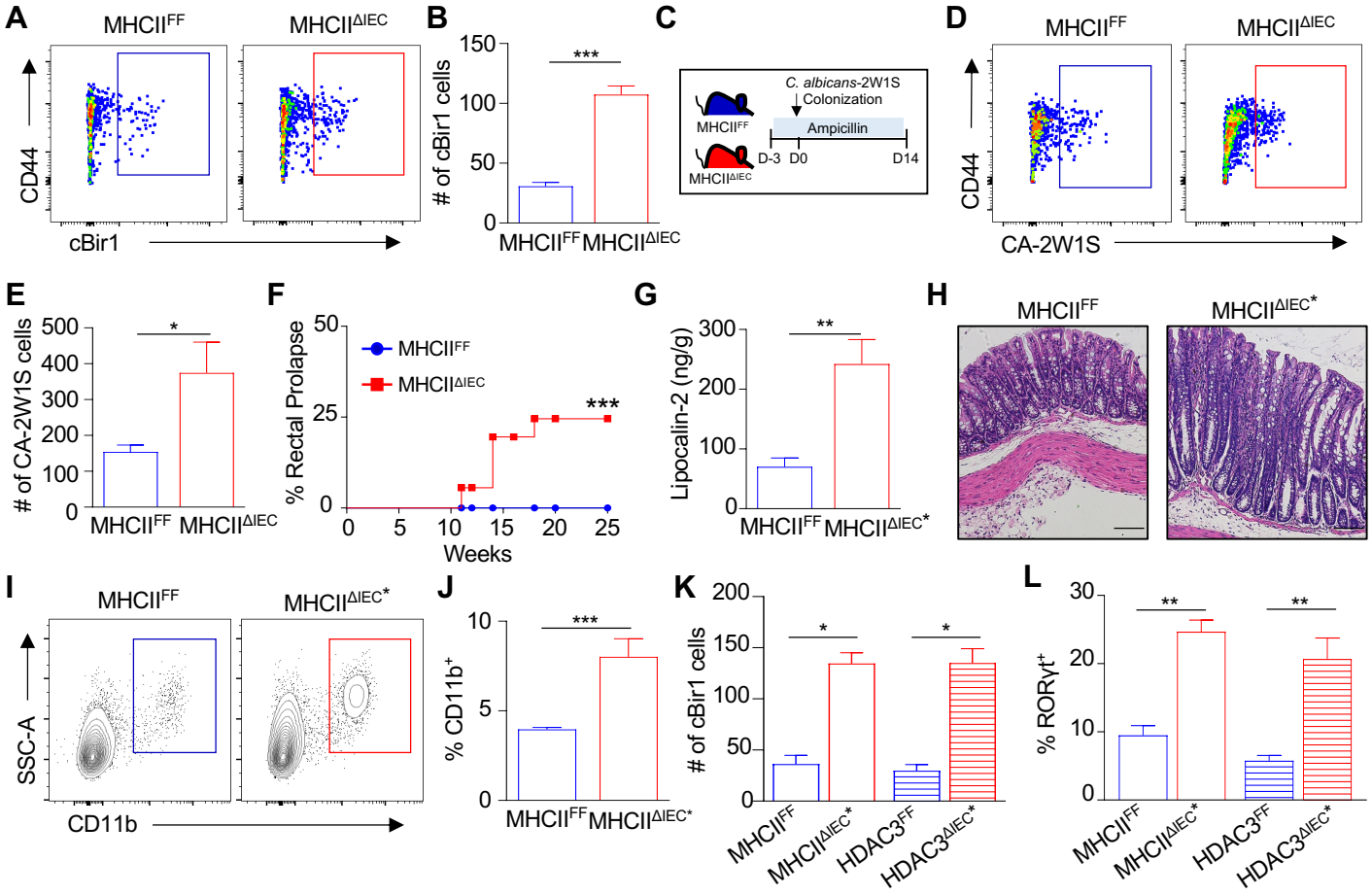

Figure. 4. Epithelial MHCII limits commensal-specific CD4+ T cells and intestinal inflammation. (**A, B**) Number of cBir1+-specific CD4+ T cells in large intestine of MHCII^{FF} and MHCII$^{\Delta IEC}$ mice. (**C**) Diagram of 2W1S-*Candida albicans* commensal colonization. (**D, E**) Number of *C. albicans*-2W1S+-specific CD4+ cells in large intestine of MHCII^{FF} and MHCII$^{\Delta IEC}$ mice. (**F**) Frequency of rectal prolapse in MHCII^{FF} and MHCII$^{\Delta IEC}$ mice. (**G**) Lipocalin-2 levels in stool of MHCII^{FF} and prolapsed MHCII$^{\Delta IEC}$ mice (MHCII$^{\Delta IEC*}$). (**H**) H&E-stained colonic sections of MHCII^{FF} and MHCII$^{\Delta IEC*}$ mice, scale bars 20 μM. (**I, J**) Frequency of myeloid cell infiltrate in MHCII^{FF} and MHCII$^{\Delta IEC*}$ mice. (**K**) cBir1+-specific CD4+ T cells and (**L**) frequency of RORγt+ cBir1+-specific CD4+ T cells in large intestine of control and prolapsed MHCII$^{\Delta IEC}$ and HDAC3$^{\Delta IEC}$ mice. Gated on live, CD45+, lineage (CD11b, B220, Ly6G, CD11c, CD8a)-, CD4+. Data are representative of at least two independent experiments, 3-6 mice per group. *p<0.05, **p<0.01, ***p<0.001.

Figure 5

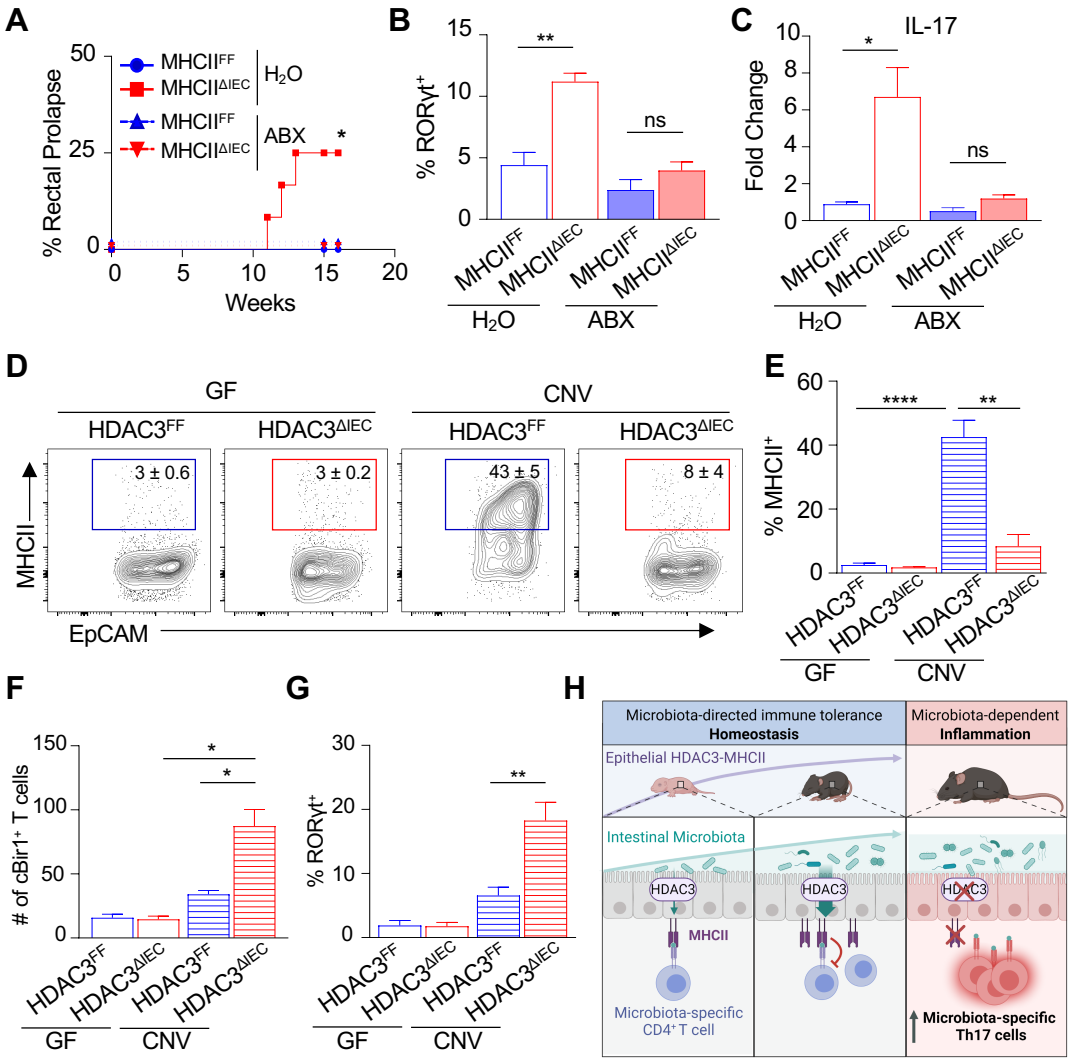

Figure. 5. HDAC3 enables microbiota to regulate epithelial dependent commensal-specific immunity. (**A**) Frequency of rectal prolapse in control and antibiotic (ABX)-treated MHCII^{FF} and MHCII$^{\Delta IEC}$ mice. (**B**) Frequency of RORγt^{+} cBir1^{+}-specific CD4^{+} T cells and (**C**) IL-17 mRNA expression in large intestine of control and ABX-treated MHCII^{FF} and MHCII$^{\Delta IEC}$ mice. (**D, E**) Frequency of MHCII^{+} EpCAM^{+} cells in large intestine of GF- and CNV- HDAC3^{FF} and HDAC3$^{\Delta IEC}$ mice. (**F**) Number of cBir1^{+} tetramer-specific CD4^{+} T cells and (**G**) frequency of RORγt^{+} cBir1^{+} T cells isolated from GF- and CNV- HDAC3^{FF} and HDAC3$^{\Delta IEC}$ mice. cBir1^{+} tetramer cells are gated on live, CD45^{+}, lineage (CD11b, B220, Ly6G, CD11c, CD8a)$^{-}$, CD4^{+}. (**H**) Microbiota drive self-tolerance early in life through upregulation of an epithelial HDAC3 dependent-MHCII pathway that limits commensal-specific Th17 cell accumulation and pathologic inflammation. Data are representative of or pooled from at least two independent experiments, 3-6 mice per group. *$p<0.05$, **$p<0.01$, ****$p<0.0001$, ns=not significant.